Nanoscale Phase Engineering of Niobium Diselenide

Journal:	*Chemistry of Materials*
Manuscript ID	cm-2017-03061q.R1
Manuscript Type:	Article
Date Submitted by the Author:	n/a
Complete List of Authors:	Bischoff, Felix; Technical University Munich, Auwärter, Willi; Technische Universitat Munchen, Physik-Department E20 Barth, Johannes; Technische Universitat Munchen, Physik-Department E20 Schiffrin, Agustin; Monash University, School of Physics & Astronomy Fuhrer, Michael; Monash University, Physics Weber, Bent; Nanyang Technological University, School of Physical and Mathematical Sciences

Nanoscale Phase Engineering of Niobium Diselenide

Felix Bischoff[1], Willi Auwärter[1], Johannes V. Barth[1], Agustin Schiffrin[2,3,4], Michael Fuhrer[2,3,4], and Bent Weber[2,3,4,5,*]

[1] Physik-Department E20, Technische Universität München, James-Franck-Straße 1, 85748 Garching, Germany

[2] ARC Center of Excellence in Future Low-Energy Electronics Technologies, Monash University, Victoria 3800, Australia

[3] Monash Centre for Atomically Thin Materials, Monash University, Victoria 3800, Australia

[4] School of Physics and Astronomy, Monash University, Victoria 3800, Australia

[5] School of Physical and Mathematical Sciences, Nanyang Technological University, Singapore 637371

KEYWORDS. Transition metal dichalcogenide, Niobium Diselenide, charge density waves, phase engineering, scanning tunneling microscopy

ABSTRACT: With continuing miniaturization in semiconductor microelectronics, atomically thin materials are emerging as promising candidate materials for future ultra-scaled electronics. In particular, the layered transition metal dichalcogenides (TMDs) have attracted significant attention due to the variety of their electronic properties, depending on the type of transition metal and its coordination within the crystal. Here, we use low-temperature scanning tunneling microscopy (STM) for the structural and electronic phase-engineering of the group-V TMD niobium diselenide ($NbSe_2$). By applying voltage pulses with an STM tip, we can transform the material crystal phase locally from trigonal prismatic (2H) to octahedral (1T), as confirmed by the concomitant emergence of a characteristic ($\sqrt{13}$x$\sqrt{13}$)R13.9° charge density wave (CDW) order. At 77 K atomic-resolution STM images of the junction with sub-lattice detail confirm the successful phase-engineering of the material, as we resolve the difference in the Nb coordination evidenced by a slip of the top Se plane. Different 1T-CDW intensities suggest interlayer interactions to be present in 1T-$NbSe_2$. Furthermore, a distinct voltage dependence suggests a complex CDW mechanism that does not just rely on a Star-of-David reconstruction as in the case of other 1T-TMDs. Additionally, bias pulses cause surface modifications inducing local lattice strain that favors a one-dimensional charge order (1D-CDW) over the intrinsic 3 x 3 CDW at 4.5 K for 2H-$NbSe_2$, which can be reversibly manipulated by STM.

Recent advances in the fabrication of transition metal dichalcogenide (TMD) nanodevices have impressively demonstrated their potential for future (opto-) electronics[1-3], catalysis, and energy storage[3-4]. Layered TMDs in particular, are quasi two–dimensional materials that consist of three atom thick van–der–Waals stacked layers of stoichiometry MX_2 (M: transition metal, X: chalcogen), where each layer consists of a sheet of transition metal atoms sandwiched between two chalcogen layers. Each transition metal atom is sixfold coordinated by chalcogens, assuming either trigonal prismatic (2H) or octahedral (1T) lattice structure. Indeed, it has been shown that these different polymorphs can coexist within the same sample, exhibiting atomically sharp boundaries.[5-8] Depending on the type of TMD, the two crystal phases can exhibit vastly different electronic properties, including metallic, insulating, semiconducting, or even superconducting. Substantial interest therefore exists to harness such atomically sharp homojunctions for the engineering of novel atomic-scale electronic devices.[3, 6, 9-10]

Phase-control in TMDs has been demonstrated in the past using either strain[9, 11-13], chemical intercalation with alkali metals,[2-3] heat[7, 10, 14], in-plane electric fields[14-16] or by injection of electronic charge[17-19]. Typically, one of the crystal phases is thermodynamically more stable than the other, whereby the stability is determined by the type of transition metal.[3-4] The group-V TMD niobium diselenide ($NbSe_2$) is of particular interest as its 2H phase exhibits collective low-temperature ground states in the form of charge density waves (CDWs) ($T_{CDW} \approx 34$ K)[20-21] and superconductivity (SC) ($T_C \approx 7$ K).[22] Owing to these properties, $NbSe_2$ has attracted significant attention over the years as an important model system to study the origins of these low temperature ground states and their correlation.[11, 20-21, 23-40]

Low-temperature scanning tunneling microscopy (STM) is ideally suited for the engineering and investigation of the atomically sharp phase boundaries, owing to its unique ability to not only image materials' surfaces with atomic resolution, but also to manipulate matter at the atomic scale.[5, 7, 10, 41-51] Here, we demonstrate STM-based phase engineering in $NbSe_2$ to create atomically sharp metal-insulator 2H/1T phase boundaries, which we investigate at temperatures down to 4.5 K. The creation of a 1T phase appears particularly intriguing since it is has been believed to be thermodynamically unstable in bulk form[52]. More recently, however, is was reported that 1T-$NbSe_2$ can be stabilized in nanometer scale regions of $NbSe_2$ monolayers[53].

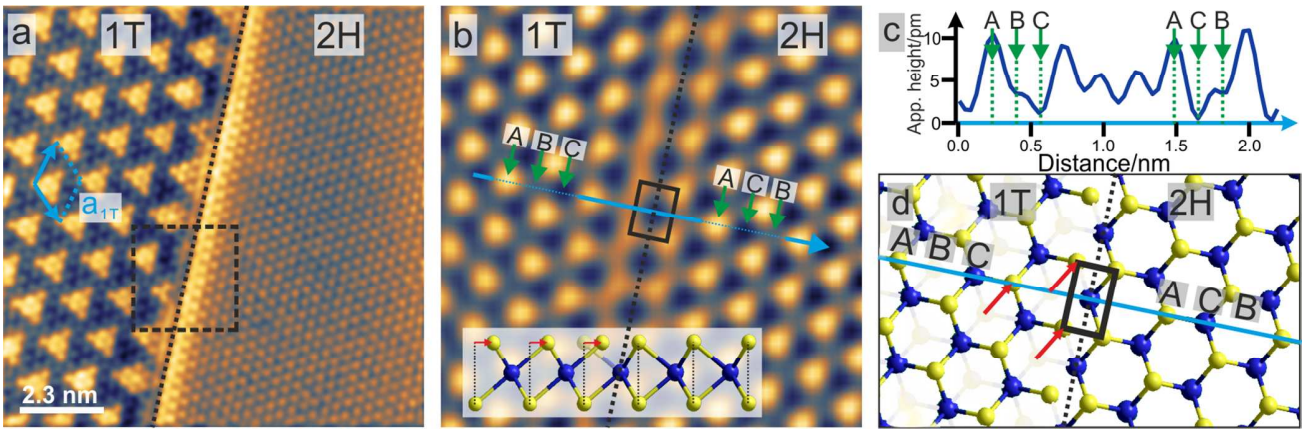

Figure 1. Atomically sharp phase boundary between 1T– and 2H–$NbSe_2$ at T = 77 K (scan parameters: I = 1.7 nA, U = –2 V). a) The pristine surface on the right does not exhibit charge modulations while a clear CDW order indicates 1T–$NbSe_2$ on the left. The charge modulation of the 1T–phase (1T–CDW) manifests as commensurate (√13x√13)R13.9° superstructure (blue arrows) with lattice constant a_{1T} = 12.4 Å. b) Close-up of the dashed square in a), showing an FFT filtered image to remove the electronic CDW modulation. Each bright dot corresponds to one selenium atom in the top Se layer. Across the boundary (black dotted line), a rectangular alignment can be clearly observed (black box). Distinct positions in the surface are highlighted by green arrows A, B and C (see text for a full description). Bottom inset: Side view of a model of one $NbSe_2$ layer. Red arrows indicate the shifted Se top plane after the 2H-1T transformation. c) Line profile along the blue line in b). Green arrows indicate lattice positions in b) correspondingly. d) A schematic of a single $NbSe_2$ layer at the phase boundary. Yellow balls represent the Se top plane that is imaged in STM, blue balls represent sub-surface Nb. Se in the bottom layer of 1T-$NbSe_2$ are shown in faded yellow. Red arrows indicate the top layer shift that leads to a rectangular Se atom arrangement at the boundary as highlighted in black. The lattice positions marked in b) and c) are labeled correspondingly.

Atomic resolution STM images of the $NbSe_2$ surface with an artificially created 1T/2H junction at 77 K are shown in Figure 1a. Due to weak van–der–Waals interlayer coupling, $NbSe_2$ cleaves between adjacent Se sheets, exposing a hexagonal chalcogen surface in the thermodynamically stable 2H phase, with a nearest neighbor distance of a = 3.44 Å along the close packed <100> directions (right hand side of Figure 1a,b, see also supporting Figure S2).[54] Here, the pristine 2H surface has been locally modified by STM bias pulses ($U_{bias} > 4$ V), resulting in regions of a commensurate (√13x√13)R13.9° CDW (left hand side of Figure 1a), several hundred square nanometers in size and lattice matched across an atomically sharp and straight boundary to the pristine 2H-$NbSe_2$ (right hand side of Figure 1a and supporting Figure S3).[7] As the data was recorded above the CDW transition temperature for 2H-$NbSe_2$ the pristine surface does not exhibit charge modulations and the occurrence of the (√13x√13)R13.9° CDW proofs a fundamental modification of the material.

We can resolve the alignment of the atomic lattices across the boundary by applying a FFT filter to remove the CDW modulation as shown in Figure 1b. The image reveals a rectangular and continuous arrangement of atoms across the 2H/1T phase boundary, resulting from a shift of the top Se plane during the 2H-1T phase transformation as indicated by red arrows in Figure 1d.[5, 7, 51]

The details of the matched lattices at the boundary are illustrated in the schematic of Figure 1d, showing the lattice structure of a single $NbSe_2$ layer after a shift of the top Se layer in the left half of the image. In this schematic we identify three distinctly different lattice sites, which we label A, B and C. A represents a Se atom (top site), B a void between Se top atoms (hollow site) and C a Nb atom within the first sub–surface sheet (hcp site). In the 2H-phase, two Se atoms from the top and bottom layers of a $NbSe_2$ monolayer are aligned on top of each other forming the trigonal prismatic coordination of the Nb center. However, in the 1T-phase, a hollow site is located above the Se atom of the sub-surface (lower) Se sheet. Following a shift of the top Se plane during phase transformation, the order of sites along the <210> crystal directions is now changed for the two phases (line-cuts of Figure 1c) and changes at the boundary.

These differences are reflected by the sub-lattice detail of our atomic resolution STM data, where we identify the top Se atom as a bright protrusion, the hollow site as a shallow depression, and the Nb hcp site as a deep depression. Following the blue line in Figure 1b from left to right, the sequence for 2H is A–B–C while for 1T it changes to A–C–B. These differences are accentuated by profiles along a <210>–direction for both phases in the FFT–filtered data. As shown in Figure 1c, the sequence of peak–shoulder–minimum switches to peak–minimum–shoulder at the phase border. Although a boundary between two 60° rotated 2H–crystals would have the same effect[55], it would fail to explain the observed electronic modulation

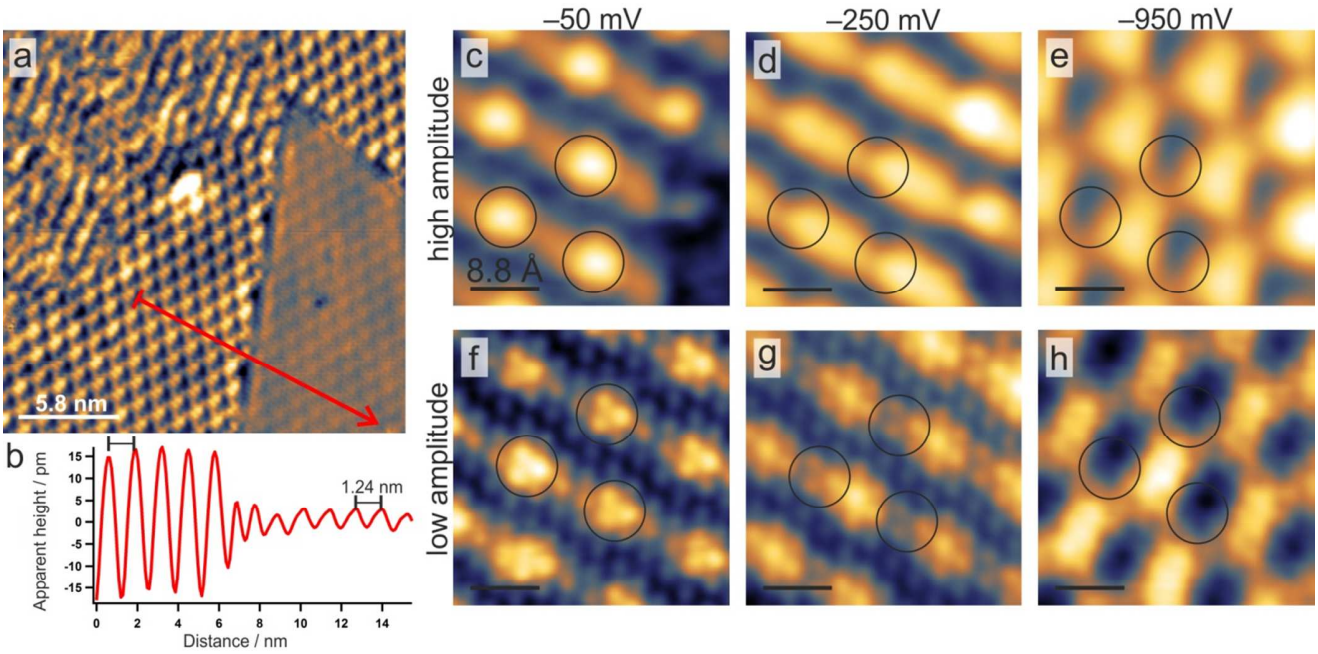

Figure 2. Characterization of the 1T–CDW at T = 77 K. a) STM topography of the boundary between areas of different 1T-CDW amplitudes. The observed 1T–CDW can occur in a disordered (top left) or highly ordered state (rest of the image) and exhibits two different amplitudes as shown by a line profile (b) along the red line in a). The wavelength is the same for both amplitudes as highlighted by the black distance indicator. c–h) STM bias dependence for both amplitudes as evidenced during constant current imaging. The first row displays the large amplitude CDW and the second row the small amplitude CDW. The STM bias is indicated above each column. Black circles mark the same position in each image and are aligned with the maximum of the CDW for –50 mV. Both rows are details from larger images across a phase boundary. Please note that the contrast in the images was adapted for best visibility of CDW features. Scan parameters: a) I = 2 nA, U = –1 V; c–h) I = 2 nA.

in the form of CDW order above T_{CDW}. The correlated differences in atomic and electronic structure across the boundary thus gives strong evidence for a successful STM-induced 2H-1T phase transformation. It should be pointed out that a recent multimethod study identified single layer 1T-$NbSe_2$ on bilayer graphene as a Mott-insulator[53], suggesting here the engineering of an atomically defined Mott-insulator-to-metal junction. Such homojunctions could be exploited in functional devices as already shown in field effect transistors made from MoS_2[6] or $MoTe_2$[56].

The observation of regions of stable 1T-$NbSe_2$ phase is surprising as it has been believed that this phase is generally thermodynamically unstable[52]. There is no report of bulk 1T-NbSe2 and only very recently, stable single-layer 1T-NbSe2 nano-flakes were synthesized.[53] Following the arguments of Wang et al.[7], we speculate that regions of 1T-$NbSe_2$ may be created by local heating via the injected STM tunneling current during the bias pulse, and then are rapidly quenched to T = 77 K which, in combination with the energetics of the 2H/1T boundary and the confinement to single and few layers, may stabilize this phase. However, additional mechanisms such as local charge injection by the STM current may play an important role. Recently, charge driven switching of the metal coordination from trigonal prismatic (2H) to octahedral (1T) was reported for $MoTe_2$[17, 19], MoS_2[17], $TaSe_2$[17], and $W_xMo_{1-x}Te_2$[17,19]. We observe no degradation of the 1T-$NbSe_2$ CDW over the course of the experiment (several hours), suggesting a CDW transition temperature in the 1T-phase above T = 77K. Indeed, previous experiments on a ($\sqrt{13}$x$\sqrt{13}$)R13.9° CDW associated with a 1T-phase were carried out at room temperature (RT) indicating a 1T–CDW transition temperature above 290 K.[41]

We observe that the 1T–CDW can exist in both a disordered (top left of Figure 2a) and an ordered phase which feature the same CDW wave vector and amplitude[7]. Furthermore, we observe that the CDW phase can exhibit different amplitudes as clearly seen on the right hand side of Figure 2a, where we find a (atomically) sharp boundary between two different CDW domains. A line profile across this boundary rules out a step edge as cause for the different contrast but instead reveals an abrupt change in CDW amplitude at the same wavelength and phase (Figure 2b). To further characterize both these CDW phases, we show the bias dependent contrast for the occupied states in Figure 2c–e (high amplitude) and Figure 2f–h (low amplitude), respectively. These data are close-ups from the same image (cf. black squares in Supporting Figure S4a) and hence were acquired with the same STM tip. Circles are centered at the location of the CDW maximum at -50 mV for reference. When decreasing the bias from –50 mV to –950 mV, the CDW maxima first continuously shift along one of the lattice vectors of the CDW and then perpendicular, resulting in a complete contrast inversion. Consequently, the maxima are located at different atoms of the $NbSe_2$ lattice for different voltages and assume different shapes. The inversion is accompanied by a change in CDW amplitude (Figure S4c). The CDW wavelength and orientation on the other hand remain constant over the whole voltage range. Interestingly, the CDW responses to bias changes are very similar for both CDW amplitudes (Figure 2 c–h and Figure S4c), suggesting that they are closely related in their origin. Furthermore, the high to low amplitude boundary seems to be atomically

smooth and does not exhibit distinct rectangular (or other) atomic arrangements (Figure S4b) suggesting the same phase (i.e. 1T-$NbSe_2$) on both sides. STM is only sensitive to the topmost TMD layer, however a 2H/1T phase transition is not limited to the top TMD sheet. It is likely to occur within several layers, creating stacks of 1T-$NbSe_2$ sheets of varying depth as well as (buried) 2H/1T interlayer boundaries. Since interlayer stacking is known to modify physical properties in TMDs,[28, 57-58] interlayer CDW stacking and/or lattice stacking may also be responsible for enhancements/attenuations of the CDW amplitude of an octahedrally coordinated first layer.

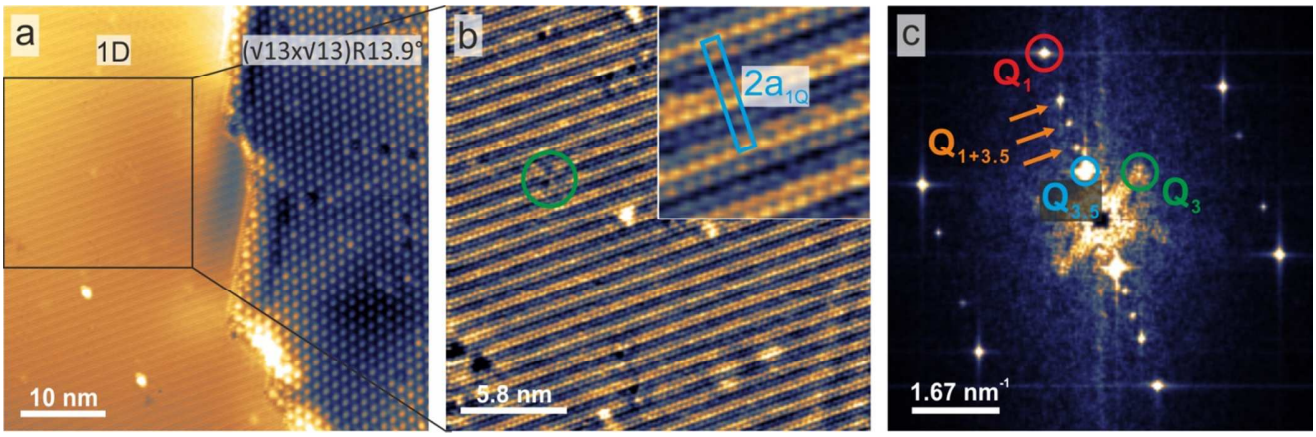

Figure 3. One dimensional CDW (1D–CDW) at the $NbSe_2$ surface at T = 4.5 K. a) In the vicinity of tip-induced surface modifications, we observe a striped (1D-) CDW. b) STM image at –200 mV of the 1D-CDW exhibiting local, short range 3x3–CDW patches within the stripe pattern (green circle). The inset shows the CDW superstructure and its unit cell. c) The corresponding FFT image reflects the periodicities of the atomic lattice (Q_1, red), the 1D–CDW ($Q_{3.5}$, blue), the 3x3–CDW (Q_3, green) as well as periodicities resulting from the superposition of the atomic lattice and the 1D–CDW ($Q_{1+3.5}$, orange). Scan parameters: a) I = 0.9 nA, U = –200mV; f) I = 2 nA, U = –50 mV.

Recently, STM studies of the TMD TaS_2 identified attenuated CDWs as buried second layer features and that changes in CDW stacking can lead to modified TMD properties.[10, 59] However, on the length scale of an interlayer distance ($d \approx 6$ Å) the tunneling current drops approximately six orders of magnitude. It therefore seems more likely that STM reproduces the effects of interlayer interactions of buried 1T-2H boundaries

Regarding Figure 2f–h, we observe that each CDW maximum always contains an identical arrangement of atoms at each bias voltage. Since wavelength and the orientation of the CDW with respect to the atomic lattice do not change, the CDW remains commensurate. 1T–TMDs such as 1T–TaS_2[10, 59-60] and 1T–$TaSe_2$[5, 61-62] have been reported to develop a Star–of–David reconstruction in the transition metal plane which is closely related to the material's electronic structure (Fermi surface nesting for 1T–TaS_2[60] and spatially localized sub-bands for $TaSe_2$[61-62]). Consequently, the CDW in these materials strictly locks to the reconstruction of the atomic lattice. As evident by the STM bias dependence, in 1T-$NbSe_2$ the CDW does not exhibit such a strict correlation with respect to the lattice. Therefore additional mechanisms are suggested besides periodic lattice distortions as a driver for the CDW formation in 1T–$NbSe_2$ such as strong (momentum–dependent) electron–phonon coupling. This is similar to the case of pristine 2H-$NbSe_2$ in which the underlying mechanism of CDW formation has been investigated for decades and still remains under intense debate. A consensus seems to exist that the driving force for CDW instabilities in 2H-$NbSe_2$ is a combined effect of lattice distortions[29-30, 32, 38] and its electronic structure leading to orbital dependent[24, 26, 36] and strong (momentum–dependent) electron–phonon coupling.[23-24, 26, 30, 36, 58, 63] The main contributions arise from the Nb plane, concerning both, lattice distortions[29] and electronic contributions of the Nb d–orbitals.[26, 29, 36, 63-64] Changes in CDW order are therefore likely related to changes in the electron-phonon coupling induced by structural variations within the Nb-plane for 2H-$NbSe_2$. In the case of 1T-$NbSe_2$, similarities in the voltage dependence to the 3x3 CDW in terms of phase and amplitude (cf. Ref [20]) also suggests strong electron-phonon coupling as the driving mechanism for CDW formation and cannot be explained by Peierls instabilities of the lattice only. The CDW formation in 1T-$NbSe_2$ therefore turns out to be more complex than for other 1T-TMDs such as 1T–TaS_2[10, 59-60] and 1T–$TaSe_2$[5, 61-62].

Finally, we investigate the CDW instability at T = 4.5 K. Here, we expect the tridirectional 3x3 CDW in pristine regions of 2H-$NbSe_2$ (Supporting Figure S2) with T_{CDW} = 34 K. In the vicinity of the phase-engineered regions, however, we observe large (> 1000 nm^2), atomically flat areas with a striped charge modulation (1D–CDW) with a smooth transition to the 3x3 CDW as shown in Figure 3a, b. The CDW propagates perpendicular to the atomic lattice along a <210> direction (Figure 3) with a 1D-CDW wavelength of a_{1D} = 3.5 ($\sqrt{3}/2$ * a) = 3.5 a*. This leads to a commensurate superstructure with doubled periodicity of 7a* perpendicular to the close-packed rows of the surface. The inset in Figure 3b is a zoom–in of the underlying image to highlight the discussed periodicities. Interestingly, small regions of local 3x3 order are discernible within the 1D-CDW pattern (green circle)

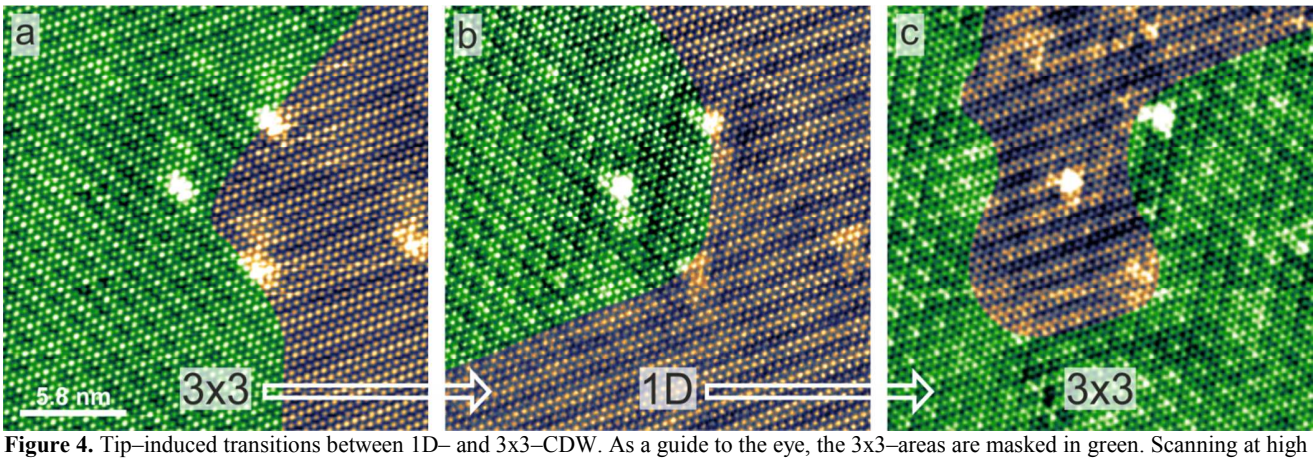

Figure 4. Tip–induced transitions between 1D– and 3x3–CDW. As a guide to the eye, the 3x3–areas are masked in green. Scanning at high bias voltages ($U > 5$ V) can reversibly transform the CDW patterns. Data recorded at 4.5 K. Scan parameters: (a) $I = 2$ nA, $U = -50$ mV; (b) $I = 2.5$ nA, $U = 50$ mV; (c) $I = 2.5$ nA, $U = 70$ mV.

as also reflected by diffuse spots Q_3 in the corresponding FFT (Figure 3c). It is likely that lattice defects are responsible for pinning the CDW, similar to what we observe in 3x3 areas above T_{CDW} (see supplementary information).[20] As the 1D stripe charge is suspected to be a strain-induced phenomenon (discussion below), this observation suggests that impurity engineering may be employed to render TMDs robust against deterioration by external influences like strain. Other spots within the FFT shown in Figure 3b correspond to the atomic lattice (Q_1, red), to the 1D–CDW ($Q_{3.5}$, blue) and to periodicities resulting from a superposition of the electronic modulation with the atomic lattice ($Q_{1+3.5}$, orange).

Previously, the 1D-CDW has been observed to exist locally confined at buckled areas with an atomically smooth interface to the 3x3 CDW of pristine $NbSe_2$[11]. Therefore, uniaxial strain in 2H-$NbSe_2$ was identified to cause an anisotropy in the electron–phonon coupling leading to transitions from tridirectional (2D) to unidirectional (1D) CDW order[11, 36]. Intriguingly, a change in the interatomic distances of as little as 0.1% (i.e. $\Delta a \approx 0.35$ pm) is sufficient to induce the transition. The magnitude of strain does not influence the CDW pattern, but always leads to the same 1D stripe structure[36]. Therefore it seems highly likely that the 1D-CDW observed in the vicinity of pulsed areas in this work is equivalent to the formerly reported "1Q"–pattern[11] at strongly buckled areas – despite the lack of evidence for strong structural distortions in our STM data.

Note that the external strain which favors the 1D-CDW likely acts uniformly on the lattice, in contrast to the periodic lattice displacements associated with the Peierls instability. Therefore a strict relationship of the charge modulation to the lattice is not given *a priori* for strain induced CDWs. Such a lock–in can however minimize the system's energy[11] and lead to a (locally) commensurate CDW from an intrinsically incommensurate CDW. The lock–in will result in phase slips of the CDW or in simultaneous adaptations of the CDW maxima and the lattice to achieve a fit.[65] To determine whether a Peierls distortion is present, we examined STM images of the occupied and unoccupied states (cf. Supporting Figure S5). A purely Peierls driven CDW should exhibit contrast inversion (for example in one-dimensional charge order in $MoSe_2$[43]). However we recognize an absence of contrast inversion that supports instead the phonon–driven scenario described for the stripe charge before.[11, 26, 36, 65]

Reversible transitions from 3x3 to 1D CDW phases may be induced by the STM tip. This is illustrated by the findings presented in Figure 4 where we demonstrate the reversible transitions between both CDW phases (3x3 and 1D). For easier identification, the 3x3–CDW regions are masked in green. Repeatedly scanning the STM-tip at comparatively high bias voltages of $U \approx 5$–6 V transforms parts of the 3x3–CDW into the 1D–CDW (Figure 4b) and finally back to the initial 3x3 CDW phase (Figure 4c). In addition, regions of the surface which were initially in 1D–CDW order (right hand side of Figure 4b) are also transformed.

The observation of reversible phase transformations between 1D– and 3x3 order underscores that (local) strain is a promising candidate to achieve phase engineering and manipulating TMD properties.[12, 66-68] The switching mechanism however remains ambiguous. Since each imaged phase represents an energetic minimum of the system, the reversible switching between two minima suggests metastability of two states close in energy. Scanning the tip at high bias might be sufficient to locally heat the sample above T_{CDW} similar to STM assisted phase switching in 1T-TaS_2[10]. Upon cooling the local pinning environment provided by the surrounding phases, defects, and local strain could favor one phase over the other. Besides a heating/cooling mechanism, charge driven phase transitions seem highly likely. For metastable ground states close in energy as observed here, the injection of charge was reported to cause switching for several TMDs[17-19]. Such phase transitions bare great promise for future applications as they can be electronically controlled via electrostatic gating[14-18, 69].

In conclusion, we have used low-temperature STM for structural and electronic phase-engineering of the group-V transition metal dichalcogenide $NbSe_2$. By applying bias pulses with an STM tip, we demonstrate that we can switch the coordination of the niobium atom from a trigonal prismatic (2H) to octahedral (1T) lattice, whereby we identify the 1T-phase by its characteristic $(\sqrt{13}x\sqrt{13})R13.9°$ charge density wave (CDW) order at temperatures down to $T = 4.5$ K. Atomic-resolution STM images of the atomically sharp and lattice matched phase boundary corroborate the successful TMD phase-engineering, supported by the observation of concomitant changes in both atomic and associated electronic structure across the junction. Different 1T-CDW amplitudes were reported for the first time to hint the 2H-1T transition to

be a few-layer phenomenon where interlayer interactions may determine the CDW amplitude. The electronic properties of 2H-$NbSe_2$ was furthermore reversibly modified between its intrinsic 3x3- and a 1D-CDW by the STM tip. For the mechanisms of the phase transformation, we have discussed different possible contributing factors, including temperature changes as well as charge injection by the STM tip. And whilst the precise mechanism of the phase changes is not known and warrants further investigation, the engineering of atomically sharp phase boundaries in transition metal dichalcogenides with substantially different electronic properties may promises their use for future atomically small electronic devices.

All experiments were performed in a commercial ultra-high vacuum chamber housing a slider-type STM by CreaTec. The STM was operated at 77 K and 4.5 K. The base pressure during the experiments was below 3×10^{-10} mbar. The $NbSe_2$ sample was either prepared by ex-situ tape exfoliation or by in-situ cleaving. When exfoliated in ambient conditions, the sample was transferred within seconds into a UHV load-lock and immediately pumped. All STM images were recorded in constant current mode. The tip was prepared by field emission and controlled dipping into an Au(111) substrate as well as by voltage pulsing on $NbSe_2$. The phase transformation from 2H- to 1T-NbSe2 was realized by pulsing the bias voltage from the scan setpoint to values exceeding 4 V for 100 ms. The tip feedback was switched off during the pulse, i.e. the tip was stabilized at the scan parameters. For the reversible switching of charge order from 3x3- to 1D-CDW, the STM feedback was kept on and the bias was increased to 5 - 6 V during scanning. The area of interest was scanned for several scan frames at elevated bias before resuming to the initial scan parameters. In the figure captions voltage *U* refers to the bias voltage applied to the sample. Gwyddion software[70] (www.gwyddion.net) was used to process the STM raw data.

AUTHOR INFORMATION

Corresponding Author

* b.weber@ntu.edu.sg

Author Contributions

FB and BW acquired the STM data. All authors discussed the data and wrote the manuscript. BW conceived and supervised the project.

ACKNOWLEDGMENT

FB acknowledges support by DAAD through a short stipend. WA acknowledges support by the Deutsche Forschungsgemeinschaft via a Heisenberg professorship and funding from the European Research Council Consolidator Grant NanoSurfs (No. 615233). MSF acknowledges support from ARC (DP150103837). BW acknowledges an Australian Research Council (ARC) DECRA fellowship (DE160101334) and a Singapore National Research Foundation (NRF) Fellowship.

ASSOCIATED CONTENT

Supporting Information

The Supporting Information is available free of charge on the ACS Publications website at DOI: […]

Visualization of $NbSe_2$ crystal structure; Atomic-resolution STM of pristine 2H-$NbSe_2$ comparing 77K and 4.5K; $NbSe_2$ after STM-based nanostructuring; Characterization of the 1T-CDW amplitude; STM bias dependence of the 1D-CDW.

REFERENCES

1. Wang, Q. H.; Kalantar-Zadeh, K.; Kis, A.; Coleman, J. N.; Strano, M. S., Electronics and optoelectronics of two-dimensional transition metal dichalcogenides. *Nature Nanotechnology* **2012,** *7*, 699-712.
2. Wang, H.; Yuan, H.; Hong, S. S.; Li, Y.; Cui, Y., Physical and chemical tuning of two-dimensional transition metal dichalcogenides. *Chemical Society Reviews* **2015,** *44*, 2664-2680.
3. Voiry, D.; Mohite, A.; Chhowalla, M., Phase engineering of transition metal dichalcogenides. *Chemical Society Reviews* **2015,** *44*, 2702-2712.
4. Chhowalla, M.; Shin, H. S.; Eda, G.; Li, L.-J.; Loh, K. P.; Zhang, H., The chemistry of two-dimensional layered transition metal dichalcogenide nanosheets. *Nature Chemistry* **2013,** *5*, 263-275.
5. Zhang, J.; Liu, J.; Huang, J. L.; Kim, P.; Lieber, C. M., Creation of Nanocrystals Through a Solid-Solid Phase Transition Induced by an STM Tip. *Science* **1996,** *274*, 757-760.
6. Kappera, R.; Voiry, D.; Yalcin, S. E.; Branch, B.; Gupta, G.; Mohite, A. D.; Chhowalla, M., Phase-engineered low-resistance contacts for ultrathin MoS_2 transistors. *Nature Materials* **2014,** *13*, 1128-1134.
7. Wang, H.; Lee, J.; Dreyer, M.; Barker, B. I., A scanning tunneling microscopy study of a new superstructure around defects created by tip–sample interaction on 2H-$NbSe_2$. *Journal of Physics: Condensed Matter* **2009,** *21*, 265005.
8. Komori, F.; Iwaki, T.; Hattori, K.; Shiino, O.; Hasegawa, T., New Superstructure on the Surface of 2H-$NbSe_2$ and Tunneling Spectra at 4.2 K. *Journal of the Physical Society of Japan* **1997,** *66*, 298-301.
9. Lin, Y.-C.; Dumcenco, D. O.; Huang, Y.-S.; Suenaga, K., Atomic mechanism of the semiconducting-to-metallic phase transition in single-layered MoS_2. *Nature Nanotechnology* **2014,** *9*, 391-396.
10. Ma, L.; Ye, C.; Yu, Y.; Lu, X. F.; Niu, X.; Kim, S.; Feng, D.; Tománek, D.; Son, Y.-W.; Chen, X. H.; Zhang, Y., A metallic mosaic phase and the origin of Mott-insulating state in 1T-TaS_2. *Nature Communications* **2016,** *7*, 10956.
11. Soumyanarayanan, A.; Yee, M. M.; He, Y.; Wezel, J. v.; Rahn, D. J.; Rossnagel, K.; Hudson, E. W.; Norman, M. R.; Hoffman, J. E., Quantum phase transition from triangular to stripe charge order in $NbSe_2$. *Proceedings of the National Academy of Sciences* **2013,** *110*, 1623-1627.
12. Duerloo, K.-A. N.; Li, Y.; Reed, E. J., Structural phase transitions in two-dimensional Mo- and W-dichalcogenide monolayers. *Nature Communications* **2014,** *5*, 4214.
13. Bhattacharyya, S.; Singh, A. K., Semiconductor-metal transition in semiconducting bilayer sheets of transition-metal dichalcogenides. *Physical Review B* **2012,** *86*, 075454.
14. Yoshida, M.; Suzuki, R.; Zhang, Y.; Nakano, M.; Iwasa, Y., Memristive phase switching in two-dimensional 1T-TaS_2 crystals. *Science Advances* **2015,** *1*, e1500606.
15. Yoshida, M.; Zhang, Y.; Ye, J.; Suzuki, R.; Imai, Y.; Kimura, S.; Fujiwara, A.; Iwasa, Y., Controlling charge-density-wave states in nano-thick crystals of 1T-TaS_2. *Scientific Reports* **2014,** *4*, srep07302.
16. Tsen, A. W.; Hovden, R.; Wang, D.; Kim, Y. D.; Okamoto, J.; Spoth, K. A.; Liu, Y.; Lu, W.; Sun, Y.; Hone, J. C.; Kourkoutis, L. F.; Kim, P.; Pasupathy, A. N., Structure and control of charge density waves in two-dimensional 1T-TaS_2.

Proceedings of the National Academy of Sciences **2015,** *112*, 15054-15059.

17. Li, Y.; Duerloo, K.-A. N.; Wauson, K.; Reed, E. J., Structural semiconductor-to-semimetal phase transition in two-dimensional materials induced by electrostatic gating. *Nature Communications* **2016,** *7*, ncomms10671.

18. Vaskivskyi, I.; Mihailovic, I. A.; Brazovskii, S.; Gospodaric, J.; Mertelj, T.; Svetin, D.; Sutar, P.; Mihailovic, D., Fast non-thermal switching between macroscopic charge-ordered quantum states induced by charge injection. *Nature Communications* **2016,** *7*, 11442.

19. Zhang, C.; KC, S.; Nie, Y.; Liang, C.; Vandenberghe, W. G.; Longo, R. C.; Zheng, Y.; Kong, F.; Hong, S.; Wallace, R. M.; Cho, K., Charge Mediated Reversible Metal–Insulator Transition in Monolayer $MoTe_2$ and $W_xMo_{1-x}Te_2$ Alloy. *ACS Nano* **2016,** *10*, 7370-7375.

20. Arguello, C. J.; Chockalingam, S. P.; Rosenthal, E. P.; Zhao, L.; Gutiérrez, C.; Kang, J. H.; Chung, W. C.; Fernandes, R. M.; Jia, S.; Millis, A. J.; Cava, R. J.; Pasupathy, A. N., Visualizing the charge density wave transition in 2H-$NbSe_2$ in real space. *Physical Review B* **2014,** *89*, 235115.

21. Chatterjee, U.; Zhao, J.; Iavarone, M.; Di Capua, R.; Castellan, J. P.; Karapetrov, G.; Malliakas, C. D.; Kanatzidis, M. G.; Claus, H.; Ruff, J. P. C.; Weber, F.; van Wezel, J.; Campuzano, J. C.; Osborn, R.; Randeria, M.; Trivedi, N.; Norman, M. R.; Rosenkranz, S., Emergence of coherence in the charge-density wave state of 2H-$NbSe_2$. *Nature Communications* **2015,** *6*, 6313.

22. Revolinsky, E.; Spiering, G. A.; Beerntsen, D. J., Superconductivity in the niobium-selenium system. *Journal of Physics and Chemistry of Solids* **1965,** *26*, 1029-1034.

23. Weber, F.; Hott, R.; Heid, R.; Bohnen, K.-P.; Rosenkranz, S.; Castellan, J.-P.; Osborn, R.; Said, A. H.; Leu, B. M.; Reznik, D., Optical phonons and the soft mode in 2H-$NbSe_2$. *Physical Review B* **2013,** *87*, 245111.

24. Weber, F.; Rosenkranz, S.; Castellan, J.-P.; Osborn, R.; Hott, R.; Heid, R.; Bohnen, K.-P.; Egami, T.; Said, A. H.; Reznik, D., Extended Phonon Collapse and the Origin of the Charge-Density Wave in 2H-$NbSe_2$. *Physical Review Letters* **2011,** *107*, 107403.

25. Koley, S.; Mohanta, N.; Taraphder, A., The unusual normal state and charge-density-wave order in 2H-$NbSe_2$. *Journal of Physics: Condensed Matter* **2015,** *27*, 185601.

26. Flicker, F.; van Wezel, J., Charge order from orbital-dependent coupling evidenced by $NbSe_2$. *Nature Communications* **2015,** *6*, 7034.

27. Zhu, X.; Cao, Y.; Zhang, J.; Plummer, E. W.; Guo, J., Classification of charge density waves based on their nature. *Proceedings of the National Academy of Sciences* **2015,** *112*, 2367-2371.

28. Xi, X.; Wang, Z.; Zhao, W.; Park, J.-H.; Law, K. T.; Berger, H.; Forró, L.; Shan, J.; Mak, K. F., Ising pairing in superconducting $NbSe_2$ atomic layers. *Nature Physics* **2016,** *12*, 139-143.

29. Malliakas, C. D.; Kanatzidis, M. G., Nb–Nb Interactions Define the Charge Density Wave Structure of 2H-$NbSe_2$. *Journal of the American Chemical Society* **2013,** *135*, 1719-1722.

30. Johannes, M. D.; Mazin, I. I., Fermi surface nesting and the origin of charge density waves in metals. *Physical Review B* **2008,** *77*, 165135.

31. Johannes, M. D.; Mazin, I. I.; Howells, C. A., Fermi-surface nesting and the origin of the charge-density wave in $NbSe_2$. *Physical Review B* **2006,** *73*, 205102.

32. Silva-Guillén, J. A.; Ordejón, P.; Guinea, F.; Canadell, E., Electronic structure of 2H- $NbSe_2$ single-layers in the CDW state. *arXiv:1603.09072 [cond-mat]* **2016**.

33. Shen, D. W.; Zhang, Y.; Yang, L. X.; Wei, J.; Ou, H. W.; Dong, J. K.; Xie, B. P.; He, C.; Zhao, J. F.; Zhou, B.; Arita, M.; Shimada, K.; Namatame, H.; Taniguchi, M.; Shi, J.; Feng, D. L., Primary Role of the Barely Occupied States in the Charge Density Wave Formation of $NbSe_2$. *Physical Review Letters* **2008,** *101*, 226406.

34. Borisenko, S. V.; Kordyuk, A. A.; Zabolotnyy, V. B.; Inosov, D. S.; Evtushinsky, D.; Büchner, B.; Yaresko, A. N.; Varykhalov, A.; Follath, R.; Eberhardt, W.; Patthey, L.; Berger, H., Two Energy Gaps and Fermi-Surface ``Arcs'' in $NbSe_2$. *Physical Review Letters* **2009,** *102*, 166402.

35. Feng, Y.; Wang, J.; Jaramillo, R.; Wezel, J. v.; Haravifard, S.; Srajer, G.; Liu, Y.; Xu, Z.-A.; Littlewood, P. B.; Rosenbaum, T. F., Order parameter fluctuations at a buried quantum critical point. *Proceedings of the National Academy of Sciences* **2012,** *109*, 7224-7229.

36. Flicker, F.; van Wezel, J., Charge ordering geometries in uniaxially strained $NbSe_2$. *Physical Review B* **2015,** *92*, 201103.

37. Ugeda, M. M.; Bradley, A. J.; Zhang, Y.; Onishi, S.; Chen, Y.; Ruan, W.; Ojeda-Aristizabal, C.; Ryu, H.; Edmonds, M. T.; Tsai, H.-Z.; Riss, A.; Mo, S.-K.; Lee, D.; Zettl, A.; Hussain, Z.; Shen, Z.-X.; Crommie, M. F., Characterization of collective ground states in single-layer $NbSe_2$. *Nature Physics* **2016,** *12*, 92-97.

38. Dai, J.; Calleja, E.; Alldredge, J.; Zhu, X.; Li, L.; Lu, W.; Sun, Y.; Wolf, T.; Berger, H.; McElroy, K., Microscopic evidence for strong periodic lattice distortion in two-dimensional charge-density wave systems. *Physical Review B* **2014,** *89*, 165140.

39. Arguello, C. J.; Rosenthal, E. P.; Andrade, E. F.; Jin, W.; Yeh, P. C.; Zaki, N.; Jia, S.; Cava, R. J.; Fernandes, R. M.; Millis, A. J.; Valla, T.; Osgood, R. M.; Pasupathy, A. N., Quasiparticle Interference, Quasiparticle Interactions, and the Origin of the Charge Density Wave in 2H- $NbSe_2$. *Physical Review Letters* **2015,** *114*, 037001.

40. Noat, Y.; Silva-Guillén, J. A.; Cren, T.; Cherkez, V.; Brun, C.; Pons, S.; Debontridder, F.; Roditchev, D.; Sacks, W.; Cario, L.; Ordejón, P.; García, A.; Canadell, E., Quasiparticle spectra of 2H- $NbSe_2$. Two-band superconductivity and the role of tunneling selectivity. *Physical Review B* **2015,** *92*, 134510.

41. Ramsak, N.; van Midden, H. J. P.; Prodan, A.; Marinkovic, V.; Boswell, F. W.; Bennett, J. C., Defect-induced room-temperature modulation in $NbSe_2$. *Physical Review B* **1999,** *60*, 4513-4516.

42. Chong, M. C.; Reecht, G.; Bulou, H.; Boeglin, A.; Scheurer, F.; Mathevet, F.; Schull, G., Narrow-Line Single-Molecule Transducer between Electronic Circuits and Surface Plasmons. *Physical Review Letters* **2016,** *116*, 036802.

43. Barja, S.; Wickenburg, S.; Liu, Z.-F.; Zhang, Y.; Ryu, H.; Ugeda, M. M.; Hussain, Z.; Shen, Z.-X.; Mo, S.-K.; Wong, E.; Salmeron, M. B.; Wang, F.; Crommie, M. F.; Ogletree, D. F.; Neaton, J. B.; Weber-Bargioni, A., Charge density wave order in 1D mirror twin boundaries of single-layer $MoSe_2$. *Nature Physics* **2016,** *12*, 751-756.

44. Weber, B.; Tan, Y. H. M.; Mahapatra, S.; Watson, T. F.; Ryu, H.; Rahman, R.; Hollenberg, L. C. L.; Klimeck, G.; Simmons, M. Y., Spin blockade and exchange in Coulomb-confined silicon double quantum dots. *Nature Nanotechnology* **2014,** *9*, 430-435.

45. Weber, B.; Mahapatra, S.; Ryu, H.; Lee, S.; Fuhrer, A.; Reusch, T. C. G.; Thompson, D. L.; Lee, W. C. T.; Klimeck, G.; Hollenberg, L. C. L.; Simmons, M. Y., Ohm's Law Survives to the Atomic Scale. *Science* **2012,** *335*, 64-67.

46. Seufert, K.; Auwärter, W.; García de Abajo, F. J.; Ecija, D.; Vijayaraghavan, S.; Joshi, S.; Barth, J. V., Controlled

Interaction of Surface Quantum-Well Electronic States. *Nano Letters* **2013,** *13*, 6130-6135.
47. Auwärter, W.; Seufert, K.; Bischoff, F.; Ecija, D.; Vijayaraghavan, S.; Joshi, S.; Klappenberger, F.; Samudrala, N.; Barth, J. V., A surface-anchored molecular four-level conductance switch based on single proton transfer. *Nature Nanotechnology* **2012,** *7*, 41-46.
48. Kalff, F. E.; Rebergen, M. P.; Fahrenfort, E.; Girovsky, J.; Toskovic, R.; Lado, J. L.; Fernández-Rossier, J.; Otte, A. F., A kilobyte rewritable atomic memory. *Nature Nanotechnology* **2016,** *advance online publication*.
49. Tapasztó, L.; Dobrik, G.; Lambin, P.; Biró, L. P., Tailoring the atomic structure of graphene nanoribbons by scanning tunnelling microscope lithography. *Nature Nanotechnology* **2008,** *3*, 397-401.
50. Dubost, V.; Cren, T.; Vaju, C.; Cario, L.; Corraze, B.; Janod, E.; Debontridder, F.; Roditchev, D., Resistive Switching at the Nanoscale in the Mott Insulator Compound $GaTa_4Se_8$. *Nano Letters* **2013,** *13*, 3648-3653.
51. Kim, J.-J.; Park, C.; Yamaguchi, W.; Shiino, O.; Kitazawa, K.; Hasegawa, T., Observation of a phase transition from the T phase to the H phase induced by a STM tip in 1T-TaS_2. *Physical Review B* **1997,** *56*, R15573-R15576.
52. Kadijk, F.; Jellinek, F., On the polymorphism of niobium diselenide. *Journal of the Less Common Metals* **1971,** *23*, 437-441.
53. Nakata, Y.; Sugawara, K.; Shimizu, R.; Okada, Y.; Han, P.; Hitosugi, T.; Ueno, K.; Sato, T.; Takahashi, T., Monolayer 1T-$NbSe_2$ as a Mott insulator. *NPG Asia Materials* **2016,** *8*, e321.
54. Marezio, M.; Dernier, P. D.; Menth, A.; Hull, G. W., The crystal structure of $NbSe_2$ at 15 K. *Journal of Solid State Chemistry* **1972,** *4*, 425-429.
55. Zhou, W.; Zou, X.; Najmaei, S.; Liu, Z.; Shi, Y.; Kong, J.; Lou, J.; Ajayan, P. M.; Yakobson, B. I.; Idrobo, J.-C., Intrinsic Structural Defects in Monolayer Molybdenum Disulfide. *Nano Letters* **2013,** *13*, 2615-2622.
56. Cho, S.; Kim, S.; Kim, J. H.; Zhao, J.; Seok, J.; Keum, D. H.; Baik, J.; Choe, D.-H.; Chang, K. J.; Suenaga, K.; Kim, S. W.; Lee, Y. H.; Yang, H., Phase patterning for ohmic homojunction contact in $MoTe_2$. *Science* **2015,** *349*, 625-628.
57. He, R.; Baren, J. v.; Yan, J.-A.; Xi, X.; Ye, Z.; Ye, G.; Lu, I.-H.; Leong, S. M.; Lui, C. H., Interlayer breathing and shear modes in $NbSe_2$ atomic layers. *2D Materials* **2016,** *3*, 031008.
58. Calandra, M.; Mazin, I. I.; Mauri, F., Effect of dimensionality on the charge-density wave in few-layer 2H-$NbSe_2$. *Physical Review B* **2009,** *80*, 241108.
59. Cho, D.; Cheon, S.; Kim, K.-S.; Lee, S.-H.; Cho, Y.-H.; Cheong, S.-W.; Yeom, H. W., Nanoscale manipulation of the Mott insulating state coupled to charge order in 1T-TaS_2. *Nature communications* **2016,** *7*.
60. Rossnagel, K., On the origin of charge-density waves in select layered transition-metal dichalcogenides. *Journal of Physics: Condensed Matter* **2011,** *23*, 213001.
61. Stoltz, D.; Bielmann, M.; Bovet, M.; Schlapbach, L.; Berger, H., Tunneling evidence for spatial location of the charge-density-wave induced band splitting in 1T-$TaSe_2$. *Physical Review B* **2007,** *76*, 073410.
62. Stoltz, D.; Bielmann, M.; Schlapbach, L.; Bovet, M.; Berger, H.; Göthelid, M.; Stoltz, S. E.; Starnberg, H. I., Atomic origin of the scanning tunneling microscopy images of charge-density-waves on 1T-$TaSe_2$. *Physica B: Condensed Matter* **2008,** *403*, 2207-2210.
63. Valla, T.; Fedorov, A. V.; Johnson, P. D.; Glans, P.-A.; McGuinness, C.; Smith, K. E.; Andrei, E. Y.; Berger, H., Quasiparticle Spectra, Charge-Density Waves, Superconductivity, and Electron-Phonon Coupling in 2H- $NbSe_2$. *Physical Review Letters* **2004,** *92*, 086401.
64. Rossnagel, K.; Seifarth, O.; Kipp, L.; Skibowski, M.; Voß, D.; Krüger, P.; Mazur, A.; Pollmann, J., Fermi surface of 2H- $NbSe_2$ and its implications on the charge-density-wave mechanism. *Physical Review B* **2001,** *64*, 235119.
65. Flicker, F.; van Wezel, J., One-Dimensional Quasicrystals from Incommensurate Charge Order. *Physical Review Letters* **2015,** *115*, 236401.
66. Bissett, M. A.; Tsuji, M.; Ago, H., Strain engineering the properties of graphene and other two-dimensional crystals. *Physical Chemistry Chemical Physics* **2014,** *16*, 11124-11138.
67. Roldán, R.; Castellanos-Gomez, A.; Cappelluti, E.; Guinea, F., Strain engineering in semiconducting two-dimensional crystals. *Journal of Physics: Condensed Matter* **2015,** *27*, 313201.
68. Johari, P.; Shenoy, V. B., Tuning the Electronic Properties of Semiconducting Transition Metal Dichalcogenides by Applying Mechanical Strains. *ACS Nano* **2012,** *6*, 5449-5456.
69. Hollander, M. J.; Liu, Y.; Lu, W.-J.; Li, L.-J.; Sun, Y.-P.; Robinson, J. A.; Datta, S., Electrically Driven Reversible Insulator–Metal Phase Transition in 1T-TaS_2. *Nano Letters* **2015,** *15*, 1861-1866.
70. Nečas, D.; Klapetek, P., Gwyddion: an open-source software for SPM data analysis. *Open Physics* **2011,** *10*, 181–188.

Authors are required to submit a graphic entry for the Table of Contents (TOC) that, in conjunction with the manuscript title, should give the reader a representative idea of one of the following: A key structure, reaction, equation, concept, or theorem, etc., that is discussed in the manuscript. Consult the journal's Instructions for Authors for TOC graphic specifications.